Sesquiterpene Lactones from *Montanoa hibiscifolia* That Inhibit the Transcription Factor NF-κB[⊥]

Stefan Müller,[†] Renato Murillo,[‡] Victor Castro,[‡] Volker Brecht,[§] and Irmgard Merfort*[,†]

Institut für Pharmazeutische Wissenschaften, Lehrstuhl für Pharmazeutische Biologie, Universität Freiburg, 79104 Freiburg, Germany, Escuela de Quimica and CIPRONA, Universidad de Costa Rica, San José, Costa Rica, and Institut für Pharmazeutische Wissenschaften, Lehrstuhl für Pharmazeutische Chemie, Universität Freiburg, 79104 Freiburg, Germany

Received December 16, 2003

The reinvestigation of the aerial parts of *Montanoa hibiscifolia* afforded four new eudesmanolides (**1**−**4**), three of them with a rare endoperoxide structural element and the fourth with a rare carbonyl function. It also afforded three unusual montabibisciolides (**5**−**7**), two (**5** and **7**) of which are new natural compounds. Additionally, seven germacrolides (**8**−**10** and **12**−**15**) and one melampolide (**11**) could be isolated, including two new germacrolides (**8** and **9**). Their structures were elucidated using 1D and 2D NMR measurement as well as ESI, CIMS, and HRMS analyses. Low-energy conformations were obtained by molecular mechanics calculations. The ^{13}C NMR data of five compounds are reported for the first time. Six sesquiterpene lactones (**4**, **6**, **10**, **11**, **12**, and **14**) were investigated for their inhibitory activity on DNA binding of the transcription factor NF-κB using Jurkat T cells as well as RAW 264.7 cells. Besides the α-methylene-γ-butyrolactone moiety the epoxy group in the acyl residue might take part in the NF-κB inhibitory activity of sesquiterpene lactones.

Montanoa hibiscifolia (Benth.) Sch. Bip. (Asteraceae, tribe Heliantheae, subtribe Montanoinae), also called tree daisy, is an erect, little branched shrubby perennial originated from an area extending from Guatemala to Costa Rica.[1] It is known for the occurrence of sesquiterpene lactones (Sls) of the germacranolide type as well as the unusual montahibisciolides.[2−4] In continuation of our search for Sls with potential antiinflammatory activity we reinvestigated the aerial parts of *M. hibiscifolia* collected in Costa Rica. The lipophilic extract was separated using common column chromatography (CC) in addition to low-pressure chromatography (see Experimental Section). Bioguided fractionation using the agar plate diffusion assay with *Bacillus subtilis* as well as the electrophoretic mobility shift assay (EMSA) with the transcription factor NF-κB as molecular target led to the isolation of 15 Sls: four new eudesmanolides (**1**−**4**), three (**1**−**3**) of which contain an endoperoxide structural element; two new (**5** and **7**) and one known (**6**) montahibisciolide;[2] seven germacrolides (**8**−**10** and **12**−**15**); and one melampolide (**11**). Of these the *trans*,*trans* germacrolides **8** and **9** are new natural compounds and **15** is new for the genus *Montanoa*,[5] whereas **10** and **12**−**14** as well as the melampolide **11** have already been isolated from *M. hibiscifolia*.[2] Structure elucidation was done by means of one- and two-dimensional NMR as well as high-resolution MS analysis.

To gain further information about structure−activity relationships, the Sls **4**, **6**, **10**, **11**, **12**, and **14** were investigated in an EMSA in order to establish whether they interfere with the DNA binding of the transcription factor NF-κB in Jurkat T and in macrophage RAW 264.7 cells. NF-κB is a central mediator of the human immune response, regulating the transcription of various proinflammatory and inflammatory mediators,[6] such as the cytokines interleukin-1, -2, -6, and -8 and TNF-α, as well as genes encoding cyclooxygenase-II, nitric oxide synthase, immunoreceptors, cell adhesion molecules, or acute phase proteins.[7] Therefore, pharmacological inhibition of NF-κB in vivo could be beneficial in the treatment of inflammatory diseases.[6]

Results and Discussion

The molecular formula of compound **1**, $C_{20}H_{24}O_8$, followed from its HRCIMS (isobutane), which showed an $[M + H]^+$ at *m*/*z* 393.1544. The ^{13}C NMR spectrum displayed 20 signals, which were assigned by gHSQCR to the resonances of seven quaternary, seven CH, two CH_2, and four CH_3 carbon atoms. Five signals could readily be assigned to a 2,3-epoxy-2-methylbutyryloxy moiety.[8] The remaining 15 carbons indicated the occurrence of a sesquiterpene skeleton. The presence of an α-methylene-γ-lactone moiety was evident from ^{13}C NMR signals at δ 124.2, 138.6, and 168.7. Consequently, in the ^1H NMR spectrum two characteristic one-proton doublets appeared downfield at δ 5.72 (H-13a) and 6.31 (H-13b), both being coupled to H-7 (δ_H 3.84). The small allylic coupling between H-7 and H-13 ($J_{7,13a} = 1.8$ Hz, $J_{7,13b} = 2$ Hz)[9] together with the positive Cotton effect at 259 nm, taken from the circular dichroism spectrum, clearly indicated a *cis*-configurated α-methylene-γ-lactone ring.[10] Assignment of H-5 (δ_H 2.30) and H-8 (δ_H 5.27) was permitted by the $^1H-^1H$ COSY and gHMQCR spectra. C-8 possessed an oxygen function due to the magnitude of its downfield shift (δ_C 77.3). The large coupling constant $J_{7,8} = 7.5$ Hz agreed with an α-configuration. The correlation between H-8 and C-1′ in the gHMQCR spectrum indicated its esterfication by the 2,3-epoxy-2-methylbutyric acid. Correlations between H-5 and C-9 and between C-10 and C-14 as well as C-15 observed in the gHMQCR experiment together with the correlations in the $^1H-^1H$ COSY spectrum showed that a eudesmanolide skeleton was present. The $^1H-^1H$ COSY spectrum exhibited only a vicinal coupling of H-8 to H-7. Consequently, C-9 must be quaternary. The magnitude of its chemical shift of δ = 101.5 can be explained only when C-9 is substituted by two oxygen functions, because one oxygen group would cause a downfield shift of only approximately

[⊥] Part VI in the series Phytochemical and Biological Studies of Costa Rican Asteraceae.

* To whom correspondence should be addressed. Tel: (49) 761 203 8373. Fax: (49) 761 203 8383. E-mail: irmgard.merfort@pharmazie.uni-freiburg.de.
[†] Lehrstuhl für Pharmazeutische Biologie, Universität Freiburg.
[‡] Universidad de Costa Rica.
[§] Lehrstuhl für Pharmazeutische Chemie, Universität Freiburg.

10.1021/np034072q CCC: $27.50
Published on Web 03/17/2004

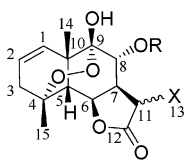

1: R = E, X = CH_2
2: R = E', X = CH_2
3: R = E', X = αH, βMe

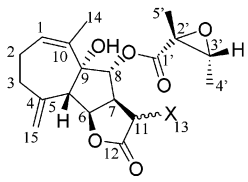

5: X = CH_2
6: X = αH, βMe

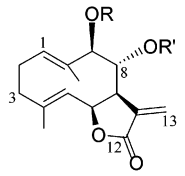

8: R = H, R' = E
9: R = H, R' = E'
10: R = E', R' = H

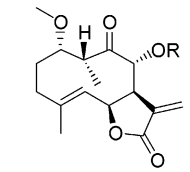

12: R = E'
13: R = E

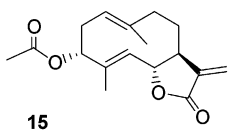

15

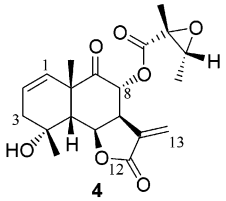

4

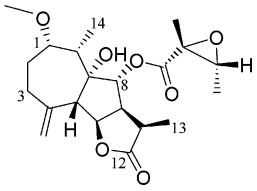

7

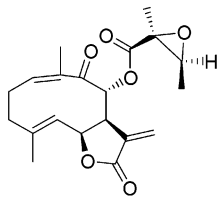

11

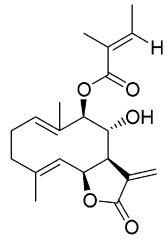

14

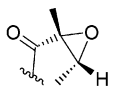

E (2′*R*,3′*R*)

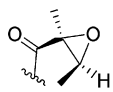

E′ (2′*S*,3′*S*)

72 ppm.[11] The signal for C-4 at $\delta = 79.4$ also indicated the presence of an oxygen function. This oxygen, together with one of those at C-9, had to be linked together in an endoperoxide structural element to be in agreement with the molecular formula. Moreover, this is the only way to stabilize the hemiacetal moiety at C-9. Endoperoxides, isolated from *Artemisia montana*,[12] showed a ^{13}C signal of the quaternary C-4 in the same range. The presence of a 1,2-double bond could be deduced from the downfield signals at $\delta = 130.9$ and 130.5 and from the correlations of C-1 with H-14 noticed in the gHMQCR spectrum. The relative configuration of the stereocenters was established by the magnitude of the coupling constants and by a NOESY experiment (see Table 1 and Figure 1). In addition, the relative configuration of all chiral centers of the eudesmanolide skeleton was confirmed by molecular modeling. The low-energy conformation of **1** (Figure 1) was obtained by molecular mechanics calculations using the conformational search option of Hyperchem, and the coupling constants ($J_{5,6} = 2.56$ Hz; $J_{6,7} = 7.03$ Hz; $J_{7,8} = 7.78$ Hz) were calculated with the PCMODEL program. These were in good agreement with the experimental values ($J_{5,6} = 1.5$ Hz; $J_{6,7} = 7.9$ Hz; $J_{7,8} = 7.5$ Hz). The configuration of the ester moiety could tentatively be assigned as 2′*R*,3′*R* on the basis of the chemical shift of the C-4′-methyl group. The shift of the C-4′-methyl group matches with the results reported in the literature.[3,11,13] Zdero and Bohlmann[11] isolated a pair of diastereomeric 2,3-epoxy-2-methylbutanoates, which differed in the chemical shift of C-4′ methyl, respectively, and Herz et al.[3] as well as Gao et al.[13] established the configuration of one diastereomer by X-ray analysis.

The HRCIMS as well as the chemical shifts and coupling constants of compound **2** deduced from the $^1H-^1H$ COSY, gHSQCR, and gHMQCR spectra were almost identical to those of **1** (see Tables 1 and 2). Because the signals of H-14 and H-15 were overlapping in the ^1H NMR spectrum, measured in $CDCl_3$, the gHMQCR spectrum was additionally recorded in C_6D_6, to confirm the position of the 1,2-double bond (see Table 2). Comparing the NMR spectra taken in $CDCl_3$ slight differences were observed only for the protons of the 2,3-epoxy-2-methylbutyryloxy moiety. Accordingly, Sl **1** and **2** differed in the absolute configuration of the ester residue. Because Sl **1** was proposed to possess the 2′*R*,3′*R* configuration, Sl **2** must have the 2′*S*,3′*S* configuration. This is in accordance with data from the literature where the chemical shift of the C-4′ methyl of the *S*,*S*-diastereomer resonates at a higher field compared to that of the *R*,*R*-isomer.[11,14,15]

HRESIMS data of compound **3** indicated the molecular formula $C_{20}H_{26}O_8$. The ^1H NMR spectrum of **3** was almost identical to those of **1** and **2** (see Table 1). Only the signals of the exomethylene group were absent and were replaced by an upfield methyl doublet at $\delta = 1.27$. NMR data (^{13}C NMR, gHSQCR, and gHMQCR) confirmed the occurrence of a methyl group at C-13 ($\delta = 9.39$). Its β-orientation was indicated by a dipolar interaction (NOE) between H-11 and H-6. The C-4′-methyl group of the 2,3-epoxy-2-methylbutyryloxy moiety resonated at $\delta = 1.31$ and agreed well with the corresponding signal in Sl **2**. Therefore, compound **3** probably possesses a 2′*S*,3′*S* configuration.

The molecular formula of compound **4**, $C_{20}H_{24}O_7$, followed from its HREIMS. ^1H and ^{13}C NMR data obtained from one- and two-dimensional analysis (^1H, $^1H-^1H$ COSY, ^{13}C, gHMQCR, gHSQCR) revealed that compound **4** differed from Sl **1** only in the substitution of C-4 and C-9 (see Table 3). C-9 was also quaternary, but its chemical shift at $\delta = 204.0$ indicated a carbonyl group. Accordingly, comparing to Sl **1** the signal for C-10 ($\delta = 49.5$) shifted downfield. Instead of an endoperoxide function, C-4 carried a hydroxy group, shown by its upfield 13-C chemical shift compared to C-4 of **1**. Correlations observed in the NOESY spectrum (see Figure 1) confirmed the same configuration of the eudesmanolide skeleton as established for compounds **1**−**3**. The low-energy conformation of **4** (Figure 1) was obtained as described for **1**. Analogously to **1**, the absolute configuration of the 2′,3′-epoxy-2′-methylbutyryloxy moiety was tentatively assigned as 2′*R*,3′*R*.

The molecular formula of compound **5** was deduced as $C_{20}H_{24}O_6$ from the HRCIMS (isobutane) data at *m*/*z* 361.1653 $[M + H]^+$. ^1H NMR data agreed well with those reported for 8α-(2′-methylbutyryloxy)-9α-hydroxy-11,13-dehydromontahibisciolide,[4] except for the acyl residue, which was derived from 2′,3′-epoxy-2′-methylbutyric acid. Its absolute configuration was deduced from the chemical shift of the C-4′ methyl group and tentatively assigned as 2′*R*,3′*R*. NMR analysis including ^1H NMR, $^1H-^1H$ COSY,

Table 1. ^{1}H NMR (300 MHz) and ^{13}C NMR (75 MHz) Spectroscopic Data in $CDCl_3$ for Compounds **1** and **3**

	compound **1**			compound **3**			
position	^{13}C δ/ppm	^{1}H δ/ppm (H; mult.; J/Hz)	gHMQCR (^{13}C−^{1}H)	^{13}C δ/ppm	^{1}H δ/ppm (H; mult.; J/Hz)	gHMQCR (^{13}C−^{1}H)	NOESY (^{1}H−^{1}H)
1	130.9	6.00 (1H; ddd; 9.8, 3.3, 3.3)	H-14	131.0	6.04 (1H; ddd; 9.9, 3.4, 3.4)	H-14	H-8
2	130.5	5.45 (1H; ddd; 9.8, 2.2, 2.2)		130.7	5.42 (1H; ddd; 9.9, 2.7, 2.7)	H-14	H-14
3α[a]	40.0	2.55 (1H; ddd; 19.8, 3.3, 2.2)	H-2, H-5, H-15	40.1	2.64 (1H; ddd; 20.0, 3.4, 2.7)	H-15	H-15
3β[a]		2.45 (1H; ddd;19.8, 3.3, 2.2)			2.47 (1H; ddd; 20.0, 3.4, 2.7)		H-15
4	79.4		H-5, H-6, H-15	79.2		H-15	
5	45.9	2.30 (1H; d; 1.5)	H-14, H-15	45.5	2.34 (1H; d; 2.0)	H-15	H-14, H-15
6	75.9	5.01 (1H; dd; 1.5, 7.9)	H-5	77.0	5.01 (1H; dd; 6.4, 2.0)	H-5	H-11, H-15
7	44.8	3.84 (1H; dddd; 7.9, 7.5, 2.0, 1.8)	H-5, H-8, H-13a, H-13b	44.7	3.54 (1H; ddd; 8.7, 8.0, 6.4)	H-5, H-8, H-11	H-15
8	77.3	5.27 (1H; d; 7.5)	H-6, H-7, H-13a, H-13b, OH	71.3	5.43 (1H; d; 8.7)	H-6, H-7, H-11	H-1, H-14
9	101.5		H-5, H-8, H-14, OH	101.9		H-5, H-14	
10	38.5		H-5, H-6, H-14, OH	38.7		H-2, H-5, H-6, H-8, H-14	
11	138.6		H-7, H-8, H-13b	39.3	2.98 (1H; dq; 8.0, 7.4)		H-6
12	168.7		H-7, H-13a, H-13b	177.1		H-7, H-11, H-13	
13a	124.2	5.72 (1H; d; 1.8)		9.4	1.27 (1H; d; 7.4)	H-11	
13b		6.31 (1H; d; 2.0)					
14	22.0	1.29 (3H; s)		22.3	1.33 (3H; s)		H-2, H-5, H-8
15	23.3	1.27 (3H; s)		23.2	1.31 (3H; s)		H-3α, H-3β, H-5, H-6, H-7
1′	172.1		H-8, H-5′	170.9		H-8, H-5′	
2′	59.8		H-4′, H-5′	59.8		H-5′	
3′	60.5	3.10 (1H; q; 5.5)	H-4′, H-5′	60.4	3.04 (1H; q; 5.3)	H-4′	H-5′
4′	13.7	1.42 (3H; d; 5.5)	H-3′	13.9	1.31 (3H; d; 5.3)	H-3′	
5′	19.2	1.61 (3H; s)		19.0	1.62 (3H; s)		H-3′
OH		4.08 (1H; br s)					

[a] Assignment determined by Chemsketch calculations.

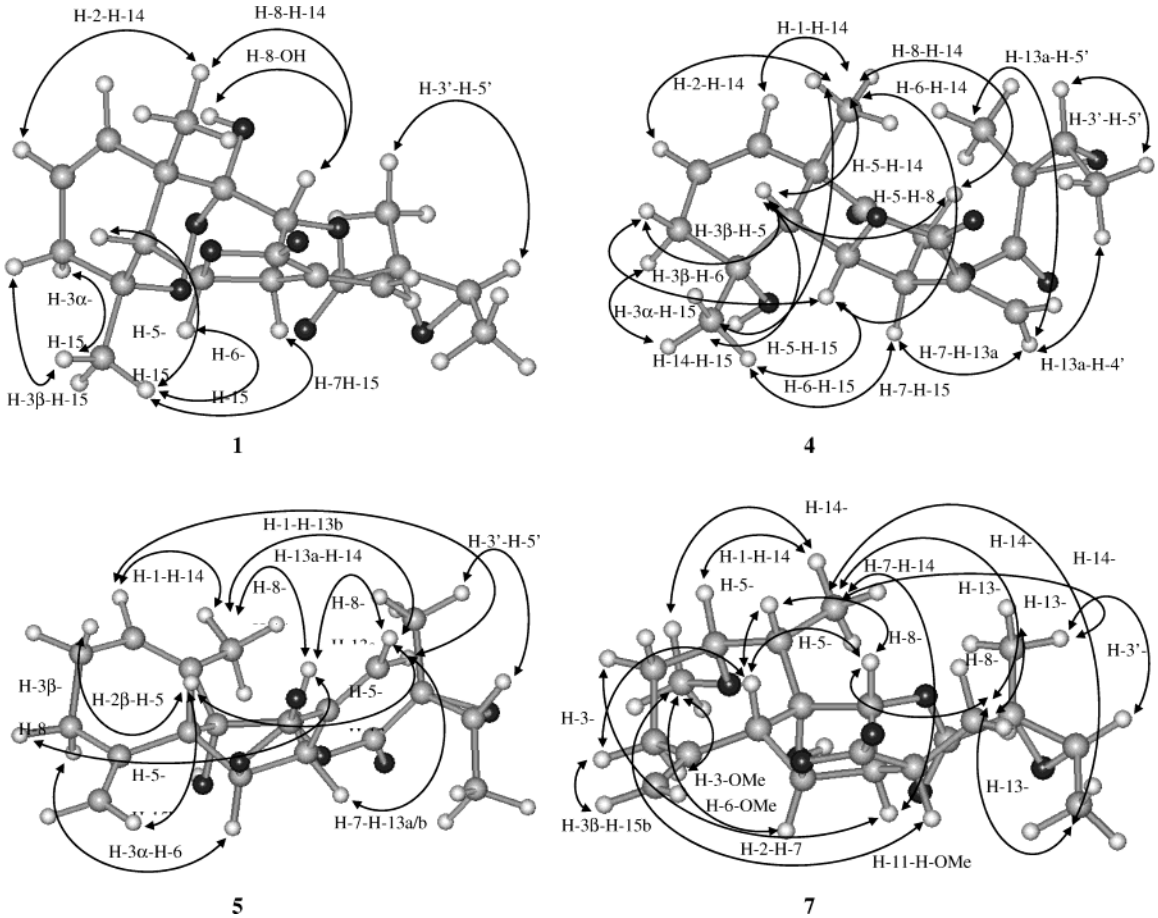

Figure 1. NOESY correlations and low-energy conformations of Sls **1**, **4**, **5**, and **7** as found by molecular mechanics calculations.

Table 2. ^{1}H NMR (300 MHz) and ^{13}C NMR (75 MHz) Spectroscopic Data for Compound **2**

	compound **2** in $CDCl_3$				compound **2** in C_6D_6		
position	^{13}C δ/ppm	^{1}H δ/ppm (H; mult.; J/Hz)	gHMQCR (^{13}C−^{1}H)	NOESY (^{1}H−^{1}H)	^{13}C δ/ppm	^{1}H δ/ppm (H; mult.; J/Hz)	gHMQCR (^{13}C−^{1}H)
1	130.7	5.97 (1H; ddd; 9.8, 3.3, 3.3)	H-14		131.2	5.54 (1H; ddd)	H-3α, H-3*β*, H-14
2	130.7	5.41 (1H; ddd; 9.8, 2.2, 2.2)		H-14, OH	130.1	5.15 (1H; ddd)	H-3α, H-3*β*, H-14
3α[a]	40.0	2.60 (1H; ddd; 19.6, 3.3, 2.2)	H-15	H-15	40.0	2.26 (1H; ddd; 19.7, 3.2, 2.4)	H-2, H-15
3*β*[a]		2.41 (1H; ddd; 19.6, 3.3, 2.2)		H-15		1.75 (1H; ddd; 19.7, 3.2, 2.4)	
4	79.5		H-5, H-15		79.0		H-3, H-5, H-15
5	45.8	2.26 (1H; d; 1.5)	H-14, H-15	H-15	45.7	1.72 (1H; d; 1.4)	H-14, H-15
6	75.8	4.80 (1H; dd; 7.9, 1.5)	H-5	H-15	75.4	4.32 (1H; dd; 7.9, 1.4)	H-5
7	45.0	3.80 (1H; dddd; 7.9, 7.3, 1.8, 1.7)	H-5, H-8, H-13a, H-13b	H-15	45.2	3.48 (1H; dddd; 7.9, 6.6, 2.0, 2.0)	H-5, H-13a, H-13b
8	77.7	5.21 (1H; d; 7.3)	H-6, H-7, H-13a, H-13b; OH	H-14, OH	78.1	5.30 (1H; d; 6.6)	H-6, H-7, H-13a, H-13b
9	101.5		H-5, H-8, H-14, OH		101.7		H-5, H-8, H-14
10	38.4		H-5, H-6, H-14, OH		38.6		H-5, H-6, H-14
11	138.6		H-7, H-8, H-13b		139.4		H-7, H-13a, H-13b
12	168.6		H-7, H-13a, H-13b		168.1		H-7, H-13a, H-13b
13a	124.4	5.70 (1H; d; 1.7)		H-5′	123.3	5.29 (1H; d; 2.0)	
13b		6.30 (1H; d; 1.8)				6.12 (1H; d; 2.0)	
14	22.1	1.24 (3H; s)		H-2, H-8	22.0	1.11 (3H; s)	
15	23.3	1.24 (3H; s)		H-3α, H-3*β*, H-5, H-6, H-7	22.9	0.59 (3H; s)	
1′	171.6		H-8, H-5′		171.5		H-8, H-5′
2′	59.8		H-4′, H-5′		59.6		H-4′, H-5′
3′	60.3	3.04 (1H; q; 5.5)	H-4′, H-5′	H-5′; H-13a	59.9	2.53 (1H; q; 5.5)	H-4′, H-5′
4′	13.9	1.29 (3H; d; 5.5)	H-3′		14.1	1.13 (3H; d; 5.5)	H-3′
5′	19.1	1.61 (3H; s)		H-3′	19.1	1.32 (3H; s)	
OH		4.26 (1H; br s)		H-2, H-8			

[a] Assignment determined by Chemsketch calculations.

Table 3. ^{1}H NMR (300 MHz) and ^{13}C NMR (75 MHz) Spectroscopic Data for Compound **4** (TMS as internal standard)

position	^{13}C δ/ppm	^{1}H δ/ppm (H; mult.; J/Hz)	gHMQCR (^{13}C−^{1}H)
1	129.2	5.75 (1H; ddd; 10.2, 1.5, 1.5)	H-5, H-14
2	123.8	5.70 (1H; ddd; 10.2, 3.5, 3.5)	
3α	39.2	2.29 (1H; ddd; 18.2, 3.5, 1.5)	H-1, H-2, H-5, H-15
3*β*		2.20 (1H; ddd; 18.2, 3.5, 1.5)	
4	70.7		H-2, H-5, H-6, H-15
5	53.7	2.64 (1H; d; 5.1)	H-1, H-14, H-15
6	75.3	4.90 (1H; dd; 5.1, 7.0)	H-5
7	44.8	3.42 (1H; dddd; 11.9, 7.0, 1.7, 1.5)	H-5, H-8, H-13a, H-13b
8	73.0	5.45 (1H; d; 11.9)	H-6, H-7, H-13a, H-13b
9	204.0		H-5, H-8, H-14
10	49.5		H-1, H-2, H-5, H-6, H-14
11	136.0		H-7, H-8, H-13b
12	167.9		H-7, H-13a, H-13b
13a	125.2	5.84 (1H; d; 1.5)	
13b		6.36 (1H; d; 1.7)	
14	27.9	1.59 (3H; s)	H-1, H-5
15	27.1	1.26 (3H; s)	H-5
1′	168.6		H-8, H-5′
2′	59.7		H-4′, H-5′
3′	60.4	3.11 (1H; q; 5.4)	H-4′, H-5′
4′	13.9	1.37 (3H; d; 5.4)	H-3′
5′	19.2	1.63 (3H; s)	

^{13}C NMR, gHMQCR, and gHSQCR also completed the existing ^{1}H NMR data of the skeleton, and the ^{13}C NMR data for this unusual skeletal type of Sl were reported for the first time (see Table 4). Low-energy conformations were calculated with Hyperchem (see Figure 1) and the coupling constants with PCMODEL. A good agreement was observed between the theoretical and the experimental coupling constants, which are given in parentheses ($J_{5,6}$ = 9.85 (9.0) Hz; $J_{6,7}$ = 8.46 (7.2) Hz; $J_{7,8}$ = 2.38 (0.5) Hz). The calculated low-energy conformation of **7** was in accordance with the reported X-ray structure of the respective 11,13-dihydroderivative[16] and showed that the central five-membered ring of the skeleton is *trans*-fused to the cycloheptene ring and *cis*-fused to the lactone ring.

Compound **6** is already known from *M. hibiscifolia*.[2] Its ^{13}C NMR data are reported for the first time (see Table 6). According to the chemical shift of the C-4′ methyl group, the absolute configuration of the acyl group should be 2′*R*,3′*R*.

Compound **7** showed in the HRCIMS the $[M + H]^+$ signal at *m*/*z* 395.2064, leading to the molecular formula, $C_{21}H_{30}O_7$. NMR data revealed a montahibisciolide skeleton. ^{1}H and ^{13}C NMR data are similar to those of **6**, except for two differences: The ^{1}H NMR spectrum of **7** exhibited a 3H singlet at δ = 3.27, indicating a methoxy group. The signals of the 1,10-double bond were missing. Thus, the methoxy group has to be located at C-1, confirmed by the correlation between OMe and H-1 in the gHMQCR spectrum. The configuration of the stereocenters C-1 and C-10 was deduced from the NOESY experiment (see Figure 1). The methoxy group exhibited an NOE with H-6, whereas H-10 showed a dipolar interaction with H-5 as well as with H-8. Therefore, a 1*S*,10*S* configuration was deduced. According to the chemical shift of C-4′ methyl, the acyl moiety must possess a 2′*R*,3′*R* configuration.

Structure elucidation of **8** and **9** was based on compound **10**. This germacrolide is known from *M. hibiscifolia*.[3] One- and two-dimensional NMR studies enable us to revise the published assignments of the ^{13}C chemical shifts for C-6, C-8, and C-9 (see Table 5).[3] Determination of the acyl

Table 4. ^{1}H NMR (300 MHz) and ^{13}C NMR (75 MHz) Spectroscopic Data in $CDCl_3$ for Compounds **5** and **7**

	compound **5**			compound **7**		
position	^{13}C δ/ppm	^{1}H δ/ppm (H; mult.; *J*/Hz)	gHMQCR (^{13}C−^{1}H)	^{13}C δ/ppm	^{1}H δ/ppm (H; mult.; *J*/Hz)	gHMQCR (^{13}C−^{1}H)
1	129.5	5.70 (1H; m)	H-14	85.6	3.36 (1H; ddd; 7.5, 1.8)	H-3, H-14, OMe
2α	24.4	2.16 (1H; m)		26.7	1.66 (1H; m; 12.4, 7.5)	H-3
2*β*		2.34 (1H; m)			2.24 (1H; dddd; 12.4, 2.0)	
3α	36.1	2.68 (1H; m)	H-15a, H-15b	31.0	2.46 (2H; m)	H-1, H-2α, H-5, H-15a, H-15b
3*β*		2.46 (1H; m)				
4	140.2		H-5	143.0		H-3, H-5, H-6
5	51.0	3.35 (1H; br d; 9.0)	H-6, H-8, H-15a,H-15b	56.7	2.73 (1H; d; 5.5)	H-3, H-15a, H-15b
6	81.9	5.25 (1H; dd; 9.0, 7.2)	H-8	82.5	4.99 (1H; dd; 8.2, 5.5)	H-5
7	48.9	3.45 (1H; dddd; 7.2, 2.4, 2.3, 0.5)	H-13a, H-13b	45.8	3.23 (1H; ddd; 9.3, 8.5, 8.2)	H-13
8	85.8	5.06 (1H; d; 0.5)	H-5	79.8	5.27 (1H; dd; 9.3, 1.1)	H-6, H-7, H-11
9	85.0		H-8, H-14	81.6		H-1, H-14
10	135.7		H-8, H-14	46.4	1.72 (1H; dq; 6.9, 1.8)	H-1, H-2α, H-14
11	135.6		H-13b	36.6	2.88 (1H; ddq; 8.5, 7.6, 1.1)	H-8, H-13
12	169.8		H-6, H-13a,b	178.3		H-7, H-11, H-13
13a	123.9	6.03 (1H; d; 2.3)		11.7	1.27 (3H; d; 7.6)	H-11
13b		6.38 (1H; d; 2.4)				
14	20.0	1.65 (3H; br s)		14.4	1.03 (3H; d; 6.9)	H-1, H-10
15a	117.1	5.29 (1H; br s)	H-5	113.2	4.95 (1H; br s)	H-3, H-5
15b		5.64 (1H; br s)			5.18 (1H; br s)	
1′	168.9		H-8, H-5′	169.2		H-8, H-5′
2′	59.2		H-4′, H-5′	59.2		H-4′, H-5′
3′	60.2	3.08 (1H; q; 5.5)	H-4′, H-5′	61.0	3.09 (1H; q, 5.5)	H-4′, H-5′
4′	13.6	1.37 (3H; d; 5.5)	H-3′	13.7	1.38 (3H; d; 5.5)	H-3′
5′	19.0	1.52 (3H; s)		19.4	1.58 (3H; s)	
OMe				57.6	3.27 (3H; s)	H-1

Table 5. ^{1}H NMR (300 MHz) and ^{13}C NMR (75 MHz) Spectroscopic Data in $CDCl_3$ for Compounds **8** and **9**

	compound **8**				compound **9**	
position	^{13}C δ/ppm	^{1}H δ/ppm (H; mult.; *J*/Hz)	gHMQCR (^{13}C−^{1}H)	NOESY	^{13}C δ/ppm	^{1}H δ/ppm (H; mult.; *J*/Hz)
1	130.5	5.63 (1H; br dd; 9.3, 5.8)	H-3a, H-3b, H-9, H-14	H-8, H-13a	130.7	5.62 (1H; m)
2	25.1	2.14−2.34 (2H; m)[a]			25.0	2.20−2.35 (2H; m)[b]
3a	38.8	2.09 (1H; m)	H-15		38.8	2.00−2.35 (2H; m)[b]
3b		2.25 (1H; m)[a]				
4	138.2		H-3a, H-6, H-15		136.4	
5	123.1	5.12 (1H; m)	H-3b, H-6, H-15		123.1	5.10−5.17 (1H; m)[b]
6	74.9	5.12 (1H; m)	H-8	H-15	75.1	5.10−5.17 (1H; m)[b]
7	46.3	3.18 (1H; m)	H-13a, H-13b	H-9, H-13a, H-14	46.4	3.19 (1H; m)
8	73.9	5.07 (1H; m; 8.6)	H-6, H-9	H-1	74.2	5.10−5.17 (1H; m)[b]
9	77.7	4.12 (1H; d; 8.6)	H-8, H-14	H-14, H-7, H-4′	78.1	4.07 (1H; d; 8.9)
10	136.6		H-9, H-14		138.2	
11	136.2		H-7, H-13a, H-13b		135.7	
12	169.7		H-7, H-13a, H-13b		169.0	
13a	126.0	5.71 (1H; d; 0.8)		H-1, H-7	126.1	5.68 (1H; d; 0.9)
13b		6.38 (1H; d; 0.8)				6.36 (1H; d; 0.8)
14	19.6	1.59 (3H; s)	H-9	H-7, H-9	19.7	1.50 (3H; s)
15	17.0	1.73 (3H; s)		H-6	17.0	1.72 (3H; s)
1′	169.1		H-8, H-5′		169.0	
2′	59.9		H-4′, H-5′		59.8	
3′	60.5	3.04 (1H; q; 5.5)	H-4′, H-5′	H-5′	60.2	3.01 (1H; q; 5.5)
4′	13.9	1.37 (3H; d; 5.5)	H-3′	H-9	14.0	1.31 (3H; d; 5.5)
5′	19.4	1.52 (3H; s)		H-3′	19.2	1.60 (3H; s)

[a] Assignment determined by gHSQCR correlations, multiplicity not determined (signal overlap). [b] Assignment determined by ^{1}H−^{1}H COSY correlations, multiplicity not determined (signal overlap).

moiety's absolute configuration was based on the chemical shift of the C-4′-methyl (δ_H = 1.32) and must be 2′*S*,3′*S*. The molecular formula of compounds **8** and **9**, $C_{20}H_{26}O_6$, followed from their HRESIMS data at *m*/*z* 385.1626 $[M + Na]^+$ for **8** and *m*/*z* 385.1625 for **9**. Their structures differed from **10** in the position of the 2,3-epoxy-2-methylbutyryloxy moiety. **8** and **9** are esterified at C-8, evidenced by a long-range coupling between C-1′ and H-8, observed in the gHMQCR spectrum. The *β*-orientation of H-8 and α-orientation of H-9 were confirmed by the NOESY experiment, which showed correlations between H-8 and H-1 and H-9 and H-7; thus the absolute configuration at these centers was 8*R*,9*R*. The methyl groups of the *trans*-configured double bonds are *syn* and below the plane of the 10-membered ring, confirmed by NOEs between H-15 and H-6α as well as H-14 and H-9α. The only difference between **8** and **9** was the configuration of the 2′,3′-epoxy group. According to the chemical shift of the C-4′ methyl, **8** should be a 2′*R*,3′*R*-epoxy-2′-methylbutanoate and **9** a 2′*S*,3′*S*-epoxy-2′-methylbutanoate.

Table 6. ^{13}C NMR Spectroscopic Data in $CDCl_3$ at 75 MHz for Compound **6** and **10**−**14**

position	6	10	11	12	13	14
1	131.1	130.6	135.9	81.4	81.4	129.4
2	25.2	25.1	23.3	26.4	26.4	25.2
3	34.9	38.8	38.1	39.1	39.1	38.9
4	143.3	137.9	140.1	142.6	142.8	135.4
5	55.4	123.4	122.1	121.0	120.9	123.4
6	81.6	75.8	75.7	74.4	74.5	68.7
7	45.0	47.1	47.3	40.8	41.2	47.5
8	78.9	68.4	69.7	70.0	70.1	82.5
9	81.5	82.9	196.2	200.3	200.4	75.7
10	136.7	134.4	137.5	47.7	47.7	138.0
11	36.0	135.4	135.9	134.7	134.5	135.1
12	179.1	169.9	168.5	169.3	168.8	170.0
13	13.5	126.7	125.4	126.5	126.6	126.5
14	20.6	19.2	20.3	7.8	7.8	19.3
14	113.0	16.9	17.2	17.1	17.1	16.9
1′	169.0	169.1	167.7	169.0	168.5	167.2
2′	59.3	59.8	59.2	59.2	59.6	128.5
3′	60.6	60.2	60.5	60.4	60.0	137.8
4′	13.7	13.9	13.7	13.4	13.9	14.4
5′	19.3	19.2	19.2	19.3	19.2	12.1
OMe				56.8	56.7	

The Sls **11**−**14**, which were identified by comparing the ^1H NMR data with those from the literature,[2] have already been isolated from *M. hibiscifolia*. Here their ^{13}C NMR data are reported for the first time (see Table 6).

Germacrolides have been mostly isolated from species within the genus *Montanoa*,[17] whereas in some species additionally heliangolides and guaianolides (e.g., in *M. tomentosa*[18]) or eudesmanolides (e.g., in *M. dumicola*[2]) have been found. The unusual montahibisciolides have been reported only from *M. hibiscifolia* and *M. leucantha* ssp. *leucantha*.[2,4] It has been discussed that this 7,5,5 tricyclic skeleton may easily be established by a transannular process from 9-oxomelampolides.[2,16] This postulated precursor was also found in *M. hibiscifolia* by us and together with the montahibisciolides in the other *Montanoa* species.[3] Melampolides and montahibisciolides have been detected only in these two species within the genus *Montanoa*, supporting the theory mentioned above. On the other hand, the absolute configuration of the 2,3-epoxy-2-methylbutanoates was likeley to be 2′*R*,3′*R* in all three montahibsciolides reported here, whereas a 2′*S*,3′*S* configuration is assigned to the suggested precursor, the 8α-(2′,3′-epoxy-2′methylbutyryloxy)-9-oxo-melampolide derivative (Sl **11**). This configurational difference indicates that the montahibisciolides ought to be naturally occurring products, as already proposed,[2] and not artifacts, arising during the isolation procedure from one another. Further studies are necessary before final conclusions can be drawn. In *M. hibiscifolia* both stereoisomers have been detected, but there is a preference for the 2′*R*,3′*R* configuration. This is in accordance with a recent report that also demonstrated a high natural stereoselectivity since the determination of the absolute configuration for 22 compounds revealed a 2*R*,3*R* configuration for 20 compounds and a 2*S*,3*S* for only two compounds.[15]

Sls **1**−**4** deserve special attention, in being the first eudesmanolides isolated from *M. hibiscifolia*. Moreover, up to now eudesmanolides with an endoperoxide structural element have been described only in *Artemisia herba-alba*,[19] and those with a carbonyl group at C-9 in *A. tournefortiana*.[20] It can be speculated whether Sl **4** serves as a precursor for **1**−**3**, from which after dehydration and cycloaddition with molecular oxygen the endoperoxides may be produced (see also Figure 2). This procedure was already discussed for the biosynthesis of 1-oxo-2α,5α-peroxyeudesm-3-en-11β*H*-12,6α-olide, the other endoperoxide with a eudesmanolide skeleton.[19] These proposed biosynthetic steps resemble the photooxidation of the guaianolide artabsin, which also results in an endoperoxide.[21] Interestingly, up to now most Sls with an endoperoxide structural element are derived from guaianolides[22] and some from xanthanolides.[23]

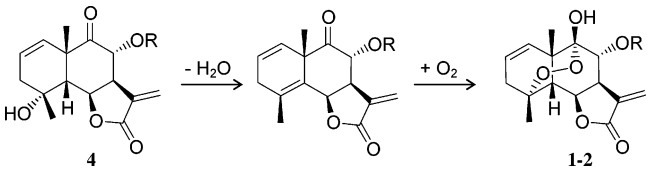

Figure 2. Hypothesis for the biogenetic origin of the Sl skeleton of compounds **1** and **2** and following hydrogenation of the exomethylene moiety of **3**.

Sls have received considerable attention due to their antiinflammatory activity.[24] We and others have recently demonstrated that they inhibit DNA binding of the transcription factor NF-κB, which is mostly composed of p50 and p65.[25,26] In recent studies we could show that they most probably inhibit NF-κB by alkylating p65 at cysteine 38,[26] besides a slight inhibition of IκB degradation, but we determined that this effect is secondary to the alkylation of p65. The subunit p65, but not p50 is responsible for transcriptional activation of the target genes.[27] There is some evidence that p65 may be involved in chronic intestinal inflammation. Therefore, therapeutic agents, such as Sls, directed at this protein might be useful.[28] A preliminary quantitative structure−activity relationship study revealed that a strong NF-κB inhibitory activity of these natural compounds correlates with the number of alkylating centers, such as the α-methylene-γ-butyrolactone and conjugated keto or aldehyde functions, but not conjugated ester groups.[29] To gain further information on structure−activity relationships, we studied some of the isolated Sls (**4**, **6**, **10**, **11**, **12**, and **14**) for their NF-κB DNA binding inhibitory activity.

Jurkat T cells, an acute T-cell leukemia cell line, were incubated with the respective Sl at various concentrations for 1 h. Total protein extracts were prepared and analyzed for NF-κB DNA binding in an electrophoretic mobility shift assay (EMSA). Stimulation with TNF-α induced novel DNA binding activity in Jurkat T cells (see Figure 3, lane 2). Antibody reactivity and competition assays identified this complex as an NF-κB p50/p65 heterodimer (data not shown, see also ref 30). All Sls with an α-methylene-γ-lactone moiety completely prevented NF-κB activation at concentrations between 10 and 100 μM (see Table 7 and Figure 3 as an example). Except for **10**, the other compounds showed slight cytotoxic effects for Jurkat cells at the highest concentration tested. Interestingly, **6**, lacking an α,β-unsaturated structural element, but possessing a reactive 2,3-epoxy-2-methylbutyryl residue inhibited NF-κB DNA binding, even though at the higher concentration of 200 μM. **4** and **12** were as active as Sls possessing two α,β-unsaturated structural elements with inhibitory concentrations of 10 and 20 μM, respectively,[29] indicating that the epoxy function of the acyl residue may contribute to the inhibitory activity besides the methylene lactone group. This may also be true for Sl **10** despite the slight reduced activity (inhibitory concentration of 50 μM). Moreover, it has to be considered whether the additional oxygen groups may favor hydrogen bonds in the vicinity of the alkylating site, thus facilitating the reaction with p65/NF-κB. Sl **14**, which possesses a tigloyl residue, inhibited NF-κB DNA binding at a 100 μM concentration. Interestingly, Sl **11**,

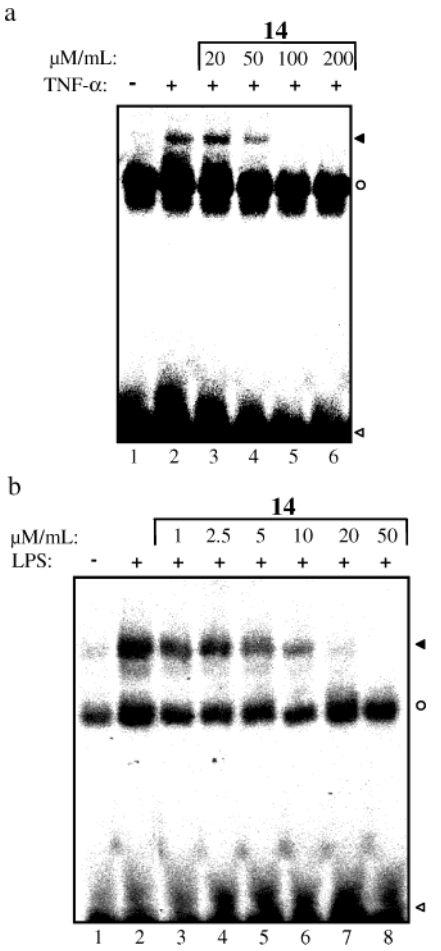

Figure 3. Effect of Sl **14** on NF-κB DNA binding in Jurkat T cells (a) and in RAW 264.7 cells (b). Lane 1 shows unstimulated control cells. In lane 2 cells were treated with 200 U/mL TNF-α (a) or 1 μg/mL LPS (b) alone. In the other lanes cells were pretreated for 1 h with various concentrations of compound **14** and subsequently stimulated with TNF-α (a) or LPS (b) for 1 h. A filled arrowhead indicates the position of NF-κB DNA complexes. The open circle denotes a nonspecific activity binding to the probe. The open arrowhead shows unbound oligonucleotide. All experiments were carried out in duplicate.

Table 7. Concentrations of Sls for a Complete Inhibition of NF-κB DNA Binding in an EMSA[a]

compound	Jurkat T cells (μM)	RAW 264.7 cells (μM)
4	10	10
6	200	n.d.
10	50	n.d.
11	50	20
12	20	10
14	100	20
parthenolide	20	n.d.

[a] Cells were pretreated with the respective Sl at the indicated concentration for 1 h prior to NF-κB stimulation with TNF-α for the Jurkat T cell line and LPS for the Raw 264.7 cells. n.d. = not determined. Parthenolide was used as control. Experiments were carried out in duplicate.

possessing two α,β-unsaturated structural elements and the epoxy function in the acyl residue, showed an unexpected lower inhibitory activity (inhibitory concentration of 50 μM).

To investigate whether the inhibition of NF-κB DNA binding depends on the cell type, Sls **4**, **11**, **12**, and **14** were also studied in Raw 264.7 cells, a monocyte-macrophage mouse cell line. Treatment was the same as described above, but LPS was used as stimulant. As expected, all Sls showed similar inhibitory properties, but mostly lower concentrations were necessary for a complete inhibition, especially pronounced with **14** (see Table 7). No cytotoxic effects were observed in RAW cells.

Altogether, our study shows for the first time that epoxy groups in acyl residues might take part in the NF-κB inhibitory activity of Sls.

Experimental Section

General Experimental Procedures. Optical rotations were measured on a polarimeter model 341 (Perkin-Elmer). Circular dichroism spectra were recorded on a CD 6 Dichrograph (JOBIN-YVON Division d'Instruments S.A.). UV spectra were determined on a UVIKON 933 UV/vis spectrophotometer (Kontron Instruments). ^{1}H NMR (300 MHz) and ^{13}C NMR (75 MHz) spectra were recorded in $CDCl_3$, using a Unity 300 (Fa. Varian) instrument. Chemical shift references were obtained by addition of TMS. MS data were taken with the following instruments. GC-EIMS: 5890 Series GC System (Agilent), 5973 Network Mass Selective Detector, 70 eV (Agilent). EIMS: MAT 8200 (Finnigan), 70 eV. CIMS and EIMS: TSQ 7000 (Finnigan). HRCIMS: MAT 95 SL (Finnigan). HRESIMS: FTQ FT (Finnigan). Medium-pressure column chromatography (MPLC) was carried out with Eurosil Bioselect 100−30, C-18 (20−45 μm), LiChroprep C-8 (25−40 μm), or LiChrospher Si 60 (12 μm), and column fractions were monitored by TLC (Si gel 60 F_{254}). For analytical HPLC a Symmetry C-8 column (4.6 × 250 mm; 5 μm) (Waters) was used. Analytical TLC was carried out with an Automatic TLC Sampler (CAMAG).

Plant Material. Aerial parts of *M. hibiscifolia* were collected in San Pedro de Montes de Oca, Costa Rica, in February 1999, and identified by L. Poveda, Professor of Botany, Universidad Nacional, Costa Rica. Voucher specimens, No. USJ 2341, are deposited at the herbarium of the University of Costa Rica.

Extraction and Isolation. Dried arial parts of *M. hibiscifolia* (1675 g) were extracted with Et_2O−MeOH (9:1). After removing the solvent the crude extract (32.4 g) was treated with MeOH at −20 °C. The soluble part (28.7 g) was fractionated by column chromatography on Sephadex LH 20 (MeOH), yielding seven fractions, which were tested for their antibacterial activity in the agar plate diffusion test using *Bacillus subtilis* as well as for their antiinflammatory activity in the NF-κB EMSA.[31] The active fraction 3 was separated on silica gel (silica gel 60, 0.063−0.200 mm, Merck), using mixtures of *n*-hexane and methyl *tert*-butyl ether (MTBE) of increasing polarity (0%, 50%, 77%, 80%). Fourteen fractions were obtained and studied in the biological assays. Isolation of the Sls followed from four subfractions. MPLC of fraction 3.7 on an RP 18 column with an increasing amount of MeOH−H_2O (35%−70%) yielded **5** (4.7 mg). A further subfraction was separated on an RP 8 column with the same conditions, obtaining **12** (94.2 mg). Separation of 3.7.3 on silica gel with *n*-hexane−EtOAc−MTBE (8:2:2) and subsequently *n*-hexane−CH_2Cl_2−EtOAc (6:5:2) yielded **13** (1.5 mg) and **15** (8.3 mg), respectively. Recrystallization of fraction 3.8 from hot MeOH led to **11** (130.7 mg, mp 144−145 °C). Subfraction 3.10 was fractionated on RP 18 with MeOH−H_2O (50%−70%), and subsequently 3.10.1 was chromatographed by MPLC on silica gel with *n*-hexane−CH_2Cl_2−EtOAc (6:5:2) in an isocratic mode, leading to **1** (5.4 mg) and **2** (5.8 mg). Fractionation of 3.10.6 in the same manner led to **14** (106.7 mg), whereas **6** (8.4 mg) and **7** (40.8 mg) were obtained from 3.10.4 using *n*-hexane−EtOAc−MTBE (8:2:2 and subsequently 6:5:2). Subfraction 3.11 was chromatographed on RP 18 with MeOH−H_2O (50%−65%) and subsequently fractionated on silica gel with MTBE−hexane (4:1) as eluent to yield **4** (22.2 mg). Further separation of 3.11.4 on silica gel with *n*-hexane−CH_2Cl_2−EtOAc (6:5:2) led to **8** (4.2 mg). Subfraction 3.12 was used for the isolation of **3** (3.2 mg) on silica gel with *n*-hexane−CH_2Cl_2−EtOAc−MTBE (5:5:2:1), as well as of **9** (11.0 mg) and **10** (80.8 mg) by *n*-hexane−EtOAc (1:1).

Cell Culture. Jurkat T cells were maintained in RPMI 1640 medium; RAW 264.7 cells, in Dulbecco's modified Eagle medium. Both were supplemented with 10% fetal calf serum and 100 IU/mL penicillin and 100 μg/mL streptomycin (all Gibco-BRL, except the antibiotics, which were from Roche).

Electrophoretic Mobility Shift Assays. Total cell extracts from Jurkat T cells or RAW 264.7 were prepared using high salt detergent buffer [Totex: 20 mM Hepes, pH 7.9, 350 mM NaCl, 20% glycerol (v/v), 1% (w/v) NP-40, 1 mM $MgCl_2$, 0.5 mM EDTA, 0.1 mM EGTA, 0.5 mM DTT, 0.1% PMSF, 1% Aprotinin]. Cells were harvested by centrifugation, washed once in ice-cold PBS (Sigma), and resuspended in four cell volumes of Totex buffer. The cell lysate was incubated on ice for 30 min, then centrifuged for 10 min at 13 000 rpm at 4 °C. The protein content of the supernatant was determined, and equal amounts of protein (10−20 μg) were added to a reaction mixture containing 20 μg of BSA (Sigma), 2 μg of poly(dI-dC) (Boehringer), 2 μL of buffer D+ (20 mM Hepes, pH 7.9; 20% glycerol, 100 mM KCl, 0.5 mM EDTA, 0.25 NP-40, 2 mM DTT, 0.1% PMSF), 4 μL of buffer F (20% Ficoll 400, 100 mM Hepes, 300 mM KCl, 10 mM DTT, 0.1% PMSF), and 100000 cpm (Cerenkov) of a ^{33}P-labeled oligonucleotide, made up to a final volume of 20 μL with distilled H_2O. Samples were incubated at room temperature for 25 min. NF-κB oligonucleotide (Promega), labeled using γ-[^{33}P]-ATP (3000 Ci/mmol; Amersham), and a T4 polynucleotide kinase (New England BioLabs) were used.

Vitality Test. The cell viability test by Trypan Blue exclusion was carried out as described in ref 32.

Calculation of the Conformations and the Coupling Constants. We generated low-energy conformations of the Sls using the conformational search option of ChemPlus (v. 2.0), which is operated under the molecular modeling package Hyperchem (v. 5.1). Energy minimizations were performed with Hyperchem's force field MM+ using the Polak-Ribiere minimization algorithm. Starting structures were created with Hyperchem and initially minimized to an RMS gradient < 0.01 kcal mol^{-1} Å^{-1}. All rotatable cyclic bonds were included as variable torsions and allowed to be changed simultaneously. The search was performed applying a usage-directed search method and standard settings for duplication tests. A search run was terminated after energy minimization of 2500 unique starting geometries. Acyl side chains of the respective Sls were not included in the conformational search. They were added manually to the most favorable Sl conformers. The resulting structures were energy minimized to an RMS gradient as above. Coupling constants were calculated with PCMODEL using the MOPAC form of the conformations created with HyperChem.

8α-(2′,3′-Epoxy-2′-methylbutyryloxy)-4α,9α-epidioxy-9*β*-hydroxy-5*βH*-eudesm-1,11(13)-dien-6*β*,12-olide (1): solid; mp dec; $[\alpha]_D^{20}$ −6° (*c* 0.049, MeOH); UV (MeOH) λ_{max} (log ϵ) 203 (4.1) nm; CD (MeOH) λ (θ) 211 (−53000), 259 (3000); ^{1}H and ^{13}C NMR, see Table 1; EIMS *m*/*z* 260 (4), 125 (26), 119 (46), 107 (100), 91 (31), 43 (64); CIMS (isobutane) *m*/*z* 393 [M + H]$^+$ (100), 375 [M + H − H_2O]$^+$ (36), 359 (50), 277 (53); HRCIMS (isobutane) *m*/*z* 393.1554 [M + H]$^+$ (calcd for $C_{20}H_{24}O_8$ + H, 393.1549).

8α-(2′,3′-Epoxy-2′-methylbutyryloxy)-4α,9α-epidioxy-9*β*-hydroxy-5*βH*-eudesm-1,11(13)-dien-6*β*,12-olide (2, diastereomer of 1): solid; mp dec; $[\alpha]_D^{20}$ +41° (*c* 0.051, MeOH); UV (MeOH) λ_{max} (log ϵ) 203 (4.1) nm; CD (MeOH) λ (θ) 213 (−54000), 259 (3000); ^{1}H and ^{13}C NMR, see Table 2; EIMS *m*/*z* 260 (4), 125 (26), 119 (38), 107 (100), 91 (32), 43 (65); HRCIMS (isobutane) *m*/*z* 393.1550 [M + H]$^+$ (calcd for $C_{20}H_{24}O_8$ + H, 393.1549).

8α-(2′,3′-Epoxy-2′-methylbutyryloxy)-4α,9α-epidioxy-9*β*-hydroxy-5*βH*-eudesm-1-en-6*β*,12-olide (3): solid; mp 198 °C; $[\alpha]_D^{20}$ +91° (*c* 0.057, MeOH); UV (MeOH) λ_{max} (log ϵ) 203 (3.9) nm; CD (MeOH) λ (θ) 216 (−6500); ^{1}H and ^{13}C NMR, see Table 1; EIMS *m*/*z* 262 (4), 173 (9), 127 (21), 119 (24), 107 (100), 91 (23), 43 (59); HRESIMS *m*/*z* 417.1524 [M + Na]$^+$ (calcd for $C_{20}H_{26}O_8$ + Na, 417.1525).

8α-(2′,3′-Epoxy-2′-methylbutyryloxy)-4α-hydroxy-9-oxo-5*βH*-eudesm-1,11(13)-dien-6*β*,12-olide (4): solid; mp 218 °C; $[\alpha]_D^{20}$ +6−7° (*c* 0.067, MeOH); UV (MeOH) λ_{max} (log ϵ) 203 (4.1) nm; CD (MeOH) λ (θ) 205 (2500), 217 (−26000), 252 (4000), 294 (−8600); ^{1}H and ^{13}C NMR, see Table 3; EIMS *m*/*z* 376 [M]$^+$ (12), 260 (11), 145 (10), 135 (13), 109 (15), 71 (16), 43 (100); CIMS (isobutane) *m*/*z* 377 [M + H]$^+$ (89), 359 (57), 263 (95), 243 (100); HREIMS *m*/*z* 376.1523 [M]$^+$ (calcd for $C_{20}H_{24}O_7$, 376.1522).

8α-(2′,3′-Epoxy-2′-methylbutyryloxy)-9α-hydroxy-(11,13)-dehydromontahibisciolide (5): gum; $[\alpha]_D^{20}$ −82° (*c* 0.050, MeOH); UV (MeOH) λ_{max} (log ϵ) 203 (4.3) nm; CD (MeOH) λ (θ) 202 (−4400), 210 (8900), 247 (1800); ^{1}H and ^{13}C NMR, see Table 4; EIMS *m*/*z* 244 (39), 173 (67), 147 (48), 119 (53), 105 (85), 91 (100), 77 (57), 55 (42); CIMS (isobutane) *m*/*z* 361 [M + H]$^+$ (41), 345 (9), 247 (52), 229 (100); HRCIMS *m*/*z* 361.1653 [M + H]$^+$ (calcd for $C_{20}H_{24}O_6$+ H, 361.1651).

8α-(2′,3′-Epoxy-2′-methylbutyryloxy)-9α-hydroxy-1α-methoxy-1,10α-dihydromontahibisciolide (7): gum; $[\alpha]_D^{20}$ +18° (*c* 0.041, MeOH); UV (MeOH) λ_{max} (log ϵ) 210 (3.6) nm; CD (MeOH) λ (θ) 203 (−7600), 225 (−4400); ^{1}H and ^{13}C NMR, see Table 4; EIMS *m*/*z* 376 [M − H_2O]$^+$ (8), 278 (15), 260 (15), 246 (18), 228 (32), 173 (39), 145 (32), 83 (58), 71 (43), 55 (52), 43 (100); CIMS (isobutane) *m*/*z* 395 [M + H]$^+$ (27), 377 (100), 261 (62), 229 (71); HRCIMS (isobutane) *m*/*z* 395.2064 [M + H]$^+$ (calcd for $C_{21}H_{30}O_7$ + H, 395.2070).

8α-(2′,3′-Epoxy-2′-methylbutyryloxy)-9*β*-hydroxygermacra-4*E*,1(10)*E*-dien-6*β*,12-olide (8): gum; UV (MeOH) λ_{max} (log ϵ) 204 (3.9) nm; CD (MeOH) λ (θ) 215 (−30000), 251 (2000); ^{1}H and ^{13}C NMR, see Tabels 5; EIMS *m*/*z* 246 (3), 213 (6), 199 (5), 185 (7), 159 (9), 121 (19), 105 (24), 91 (26), 55 (23), 43 (100); CIMS (isobutane) *m*/*z* 363 [M + H]$^+$ (41), 247 (91), 229 (100); HRESIMS *m*/*z* 385.1626 [M + Na]$^+$ (calcd for $C_{20}H_{26}O_6$ + Na, 385.1627).

8α-(2′,3′-Epoxy-2′-methylbutyryloxy)-9*β*-hydroxygermacra-4*E*,1(10)*E*-dien-6*β*,12-olide (9, diastereomer of 8): mp 190 °C; $[\alpha]_D^{20}$ −56° (*c* 0.035, MeOH); UV (MeOH) λ_{max} (log ϵ) 205 (4.0) nm; CD (MeOH) λ (θ) 199 (2000), 214.5 (−50000), 257 (1500); ^{1}H and ^{13}C NMR, see Tabels 5; EIMS *m*/*z* 246 (3), 213 (6), 200 (5), 185 (7), 159 (8), 133 (16), 121 (14), 105 (23), 91 (22), 55 (18), 43 (100); CIMS (isobutane) *m*/*z* 363 [M + H]$^+$ (27), 247 (100), 229 (79); HRESIMS *m*/*z* 385.1625 [M + Na]$^+$ (calcd for $C_{20}H_{26}O_6$ + Na, 385.1627).

Acknowledgment. The authors are grateful to the Volkswagenstiftung for financial support, to B. Schuler, Lehrstuhl für Pharmazeutische Biologie for experimental assistence, to M. Wagner, Institut für Pharmazeutische Chemie, Universität Freiburg, for recording the CD spectra and ORD spectra, to Dr. J. Wörth and C. Warth, Institut für Organische Chemie, for measuring the mass spectra, to Dr. E. Schröder, Thermo Finnigan MAT GmbH, Bremen, for recording the HRMS spectra, and to Prof. L. Poveda, Universidad Nacional, Costa Rica, for identification of *M. hibiscifolia*.

References and Notes

(1) Funk, V. A. *Mem. N. Y. Bot. Gard.* **1982**, *36*, 1−133.
(2) Bohlmann, F.; Schmeda-Hirschmann, G.; Jakupovic, J.; Castro, V.; Ciccio, J. F.; Calvo, G. *J. Nat. Prod.* **1984**, *47*, 663−672.
(3) Herz, W.; Govindan, S. V.; Blount, J. F. *J. Org. Chem.* **1980**, *45*, 1113−1116.
(4) Quijano, L.; Trejo, R. I.; Collera, O.; Rios, T. *Phytochemistry* **1994**, *36*, 1443−1448.
(5) Ortega, A.; Toscano, R. A.; Maldonado, E. *Phytochemistry* **1998**, *49*, 1085−1090.
(6) Barnes, P. J.; Karin, M. *New Engl. J. Med.* **1997**, *336*, 1066−1071.
(7) Pahl, H. L. *Oncogene* **1999**, *18*, 6853−6866.
(8) Torres-Valencia, J. M.; Cerda-Garcia-Rojas, C. M.; Joseph-Nathan, P. *Tetrahedron Asymmetry* **1998**, *9*, 757−764.
(9) Samek, Z. *Tetrahedron* **1970**, *9*, 671−676.
(10) Stöcklin, W.; Waddell, T. G.; Geissman, T. A. *Tetrahedron* **1970**, *26*, 2397−2410.
(11) Zdero, C.Bohlmann, F. *Phytochemistry* **1989**, *28*, 1433−1439.
(12) Koreeda, M.; Nagaki, M.; Hayami, K. I.; Matsueda, S. *Yakugaku Zasshi* **1988**, *108*, 434−436.
(13) Gao, F.; Wang, H.; Mabry, T. J.; Abboud, K. A.; Simonsen, S. H. *Phytochemistry* **1989**, *28*, 2409−2414.
(14) Torres-Valencia, J. M.; Cerda-Garcia-Rojas, C. M.; Roman, L. U.; Hernandez, J. D.; Joseph-Nathan, P. *Phytochemistry* **1998**, *49*, 2569−2572.

(15) Torres-Valencia, J. M.; Cerda-Garcia-Rojas, C. M.; Joseph-Nathan, P. *Phytochem. Anal.* **1999**, *10*, 221−237.
(16) Quijano, L.; Rios, T.; Toscano, R. A.; Fronczek, F. R. *J. Chem. Crystallogr.* **1996**, *26*, 753−757.
(17) Quijano, L.; Calderon, J. S.; Gomez-Garibay, F.; Bautista, S.; Rios, T.; Fronczek, F. R. *Phytochemistry* **1986**, *25*, 695−697.
(18) Lidida-Pérez, A.; Caballero, M. B. A.; Ortega, A.; Gavino, R.; Romo de Vivar, A. *Planta Med.* **1994**, *60*, 263−266.
(19) Marco, J. A.; Sanz, J. F.; Falcó, E.; Jakupovic, J.; Lex, J. *Tetrahedron* **1990**, *46*, 7941−7950.
(20) Rustaiyan, A.; Bamonieri, A.; Raffatrad, M.; Jakupovic, J.; Bohlmann, F. *Phytochemistry* **1987**, *26*, 2307−2310.
(21) Beauhaire, J.;.Fourrey, J.-L. *J. Chem. Soc., Perkin Trans. 1* **1982** 861−864.
(22) Jakupovic, J.; Chau-Thi, T. V.; Warning, U.; Bohlmann, F.; Greger, H. *Phytochemistry* **1986**, *25*, 1663−1667.
(23) Mahmoud, A. A. *Planta Med.* **1998**, *64*, 724−727.
(24) Hall, I. H.; Lee, K. H.; Starnes, C. O.; Sumida, Y.; Wu, R. Y.; Waddell, T. G.; Cochran, J. W.; Gerhart, K. G. *J. Pharm. Sci.* **1979**, *68*, 537−542.
(25) Bork, P. M.; Schmitz, M. L.; Kuhnt, M.; Escher, C.; Heinrich, M. *FEBS Lett.* **1997**, *402*, 85−90.
(26) Garcia-Pineres, A. J.; Castro, V.; Mora, G.; Schmidt, T. J.; Strunck, E.; Pahl, H. L.; Merfort, I. *J. Biol. Chem.* **2001**, *276*, 39713−39720.
(27) Karin, M.Ben-Neriah, Y. *Annu. Rev. Immunol.* **2000**, *18*, 621−663.
(28) Aradhya, S.Nelson, D. L. *Curr. Opin. Genet. Dev.* **2001**, *11*, 300−306.
(29) Rüngeler, P.; Castro, V.; Mora, G.; Goren, N.; Vichnewski, W.; Pahl, H. L.; Merfort, I.; Schmidt, T. J. *Bioorg. Med. Chem.* **1999**, *7*, 2343−2352.
(30) Pahl, H. L.Baeuerle, P. A. *EMBO J.* **1995**, *14*, 2580−2588.
(31) Lyss, G.; Schmidt, T. J.; Pahl, H. L.; Merfort, I. *Pharm. Pharmacol. Lett.* **1999**, *9*, 5−8.
(32) Ausubel, F. *Current Protocols in Molecular Biology*; John Wiley & Sons: New York, 1998; p 11.5.1.

NP034072Q